

We are IntechOpen, the world's leading publisher of Open Access books Built by scientists, for scientists

4,800

Open access books available

122,000

International authors and editors

135M

Downloads

Our authors are among the

154

Countries delivered to

TOP 1%

most cited scientists

12.2%

Contributors from top 500 universities



WEB OF SCIENCE™

Selection of our books indexed in the Book Citation Index
in Web of Science™ Core Collection (BKCI)

Interested in publishing with us?
Contact book.department@intechopen.com

Numbers displayed above are based on latest data collected.
For more information visit www.intechopen.com



Autonomous Flight Control for RC Helicopter Using a Wireless Camera

Yue Bao¹, Syuhei Saito² and Yutaro Koya¹

¹*Tokyo City University,*

²*Canon Inc.*

Japan

1. Introduction

In recent years, there are a lot of researches on the subject of autonomous flight control of a micro radio control helicopter. Some of them are about flight control of unmanned helicopter (Sugeno et al., 1996) (Nakamura et al., 2001). The approach using the fuzzy control system which consists of IF-Then control rules is satisfying the requirements for the flight control performance of an unmanned helicopter like hovering, takeoff, rotating, and landing. It is necessary to presume three dimensional position and posture of micro RC helicopter for the autonomous flight control.

A position and posture presumption method for the autonomous flight control of the RC helicopter using GPS (Global Positioning System), IMU (Inertial Measurement Unit), Laser Range Finder (Amida et al., 1998), and the image processing, etc. had been proposed. However, the method using GPS cannot be used at the place which cannot receive the electric waves from satellites. Therefore, it is a problem that it cannot be used for the flight control in a room. Although the method which uses various sensors, such as IMU and Laser Range Finder, can be used indoors, you have to arrange many expensive sensors or receivers in the room beforehand. So, these methods are not efficient. On the other hand, the method using an image inputted by a camera can be used in not only outdoors but also indoors, and is low price. However, this method needs to install many artificial markers in the surroundings, and it is a problem that the speed of the image inputting and image processing cannot catch up the speed of movement or vibration of a RC helicopter. A method presuming the three dimensional position and posture of a RC helicopter by the stereo measurement with two or more cameras installed in the ground was also proposed. In this case, the moving range of the RC helicopter is limited in the place where two or more cameras are installed. Moreover, there is a problem for which a high resolution camera must be used to cover a whole moving range. (Ohtake et al., 2009)

Authors are studying an autonomous flight of a RC helicopter with a small-wireless camera and a simple artificial marker which is set on the ground. This method doesn't need to set the expensive sensors, receivers, and cameras in the flight environment. And, we thought that a more wide-ranging flight is possible if the natural feature points are detected from the image obtained by the camera on the RC helicopter. This chapter contains the following contents.

- Input method of image from a small, wireless camera which is set on a RC helicopter.
- Extraction method of feature points from an image of flight environment taken with a camera on RC helicopter.
- Calculation method of three dimensional position and posture of RC helicopter by image processing.
- Experiment of autonomous flight of a RC helicopter using fuzzy logic control.

2. Composition of system

The overview of a micro RC helicopter with coaxial counter-rotating blades used in our experiment is shown in Fig.1. Since this RC helicopter can negate a running torque of a body by a running torque between an up propeller and a down propeller, it has the feature that it can fly without being shakier than the usual RC helicopter. The composition of our experiment system for automatic guidance of RC helicopter is shown in Fig.2. A small wireless camera is attached on the RC helicopter as shown in Fig.3, and the image of the ground is acquired with this camera, and this image is sent to the receiver on ground, and then sent to the computer through a video capture. The position and posture of the RC



Fig. 1. Micro RC helicopter with the coaxial contra-rotating rotors

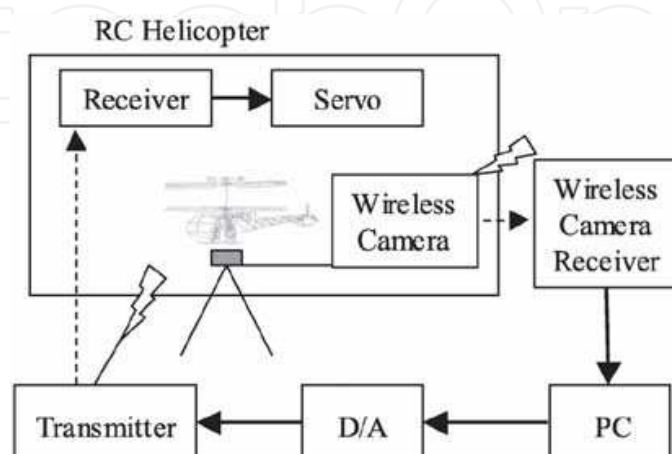


Fig. 2. Composition of automatic guidance system



Fig. 3. RC helicopter equipped with a micro wireless camera



Fig. 4. An artificial marker

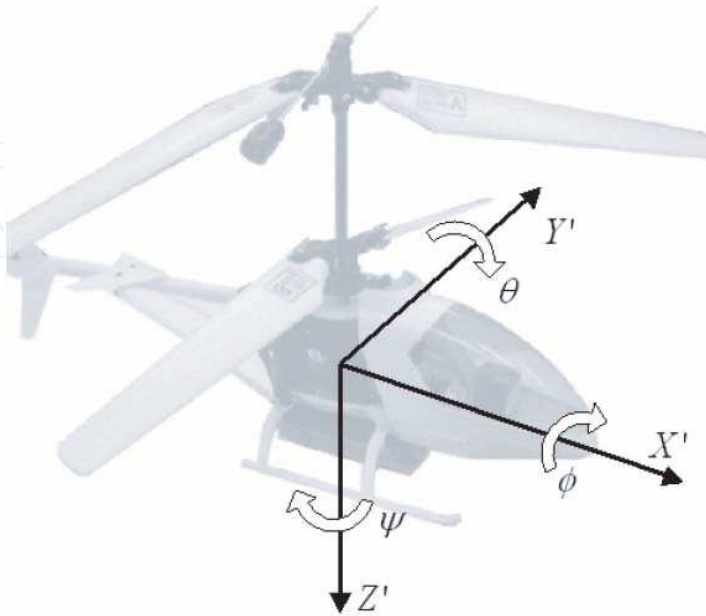


Fig. 5. Coordinate axes and attitude angles

helicopter are computed with image processing by the computer set on the ground, and, this image processing used the position and shape of an artificial marker in the camera image like Fig.4. The three dimensional position of the RC helicopter $(x(t), y(t), z(t))$ and the changing speed of the position $(\dot{x}(t), \dot{y}(t), \dot{z}(t))$ and the attitude angles $\psi(t)$ and changing speed of attitude angles $\dot{\psi}(t)$ can be obtained by this calculation. Fig.5 shows the relation between these coordinate axes and attitude angles.

This micro RC helicopter is controlled by four control signals, such as Aileron, Elevator, Rudder, and Throttle, and, the control rule of fuzzy logic control is decided by using measurement data mentioned above. The control signals are sent to micro RC helicopter through the digital-analog converter.

3. Image processing

3.1 Image input

The micro wireless camera attached on the RC helicopter takes an image by interlaces scanning. If the camera takes an image during RC helicopter flying, since the vibration of the RC helicopter is quicker than the frame rate of the camera, the image taken by the camera will be a blurred image resulting from an interlace like Fig.6. We devised a method skipping the odd number line (or, even number line) of input image to acquire an clear input image while the RC helicopter is flying.

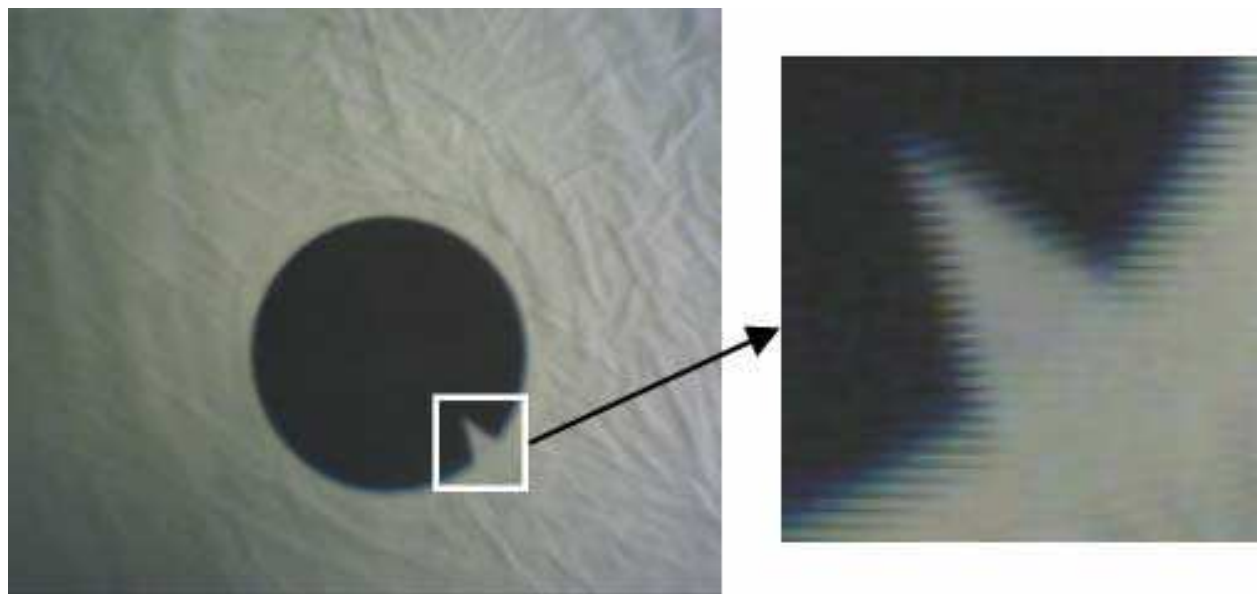


Fig. 6. A blurring image acquired by wireless camera

3.2 Feature point extraction

Feature point detection is defined in terms of local neighborhood operations applied to an image such as an edge and corner. Harris operator (Harris and Stephens, 1988) (Schmid et al., 1998) and SUSAN operator (Smith and Brady, 1997) are well known as common feature detectors. The methods (Neumann and You, 1999) (Bao and Komiya, 2008) to estimate

position and attitude by using natural feature points or marker in the input image are proposed too. Our prototype experiment system used the Harris operator which can extract the same feature points in higher rate more than other feature point extraction methods (Schmid et al., 1998). First, we obtain a grayscale image from camera. Let us consider taking an image patch over an area (u, v) from an image I and shifting it by (x, y) . The Harris matrix M can be found by taking the second derivative of the sum of squared differences between these two patches around $(x, y) = (0, 0)$. M is given by:

$$M = \begin{pmatrix} G_{\sigma} \left(\frac{\partial^2 I}{\partial^2 x} \right) & G_{\sigma} \left(\frac{\partial I}{\partial x} \frac{\partial I}{\partial y} \right) \\ G_{\sigma} \left(\frac{\partial I}{\partial x} \frac{\partial I}{\partial y} \right) & G_{\sigma} \left(\frac{\partial^2 I}{\partial^2 y} \right) \end{pmatrix} \quad (1)$$

Let the standard deviation of G in the equation be σ with Gaussian function for performing smoothing with Gaussian filter. The strength of a corner is decided by second derivative. Here, the eigenvalue of M is (λ_1, λ_2) , and the value of eigenvalue can be got from the following inference.

- If $\lambda_1 \approx 0$ and $\lambda_2 \approx 0$, then there are no features at this pixel (x, y) .
- If either λ_1 or λ_2 is large positive value, then an edge is found.
- If λ_1 and λ_2 are both large positive values, then a corner is found.

Because the exact calculation of eigenvalue by the method of Harris will increase computational amount, the following functions R were proposed instead of those calculation methods.

$$R = \det(M) - k(tr(M))^2 \quad (2)$$

$$R = \lambda_1 \lambda_2 - k(\lambda_1 + \lambda_2)^2 \quad (3)$$

The \det expresses a determinant and tr expresses the sum of the diagonal element of a matrix, and k is a value decided experientially.

The kanade-Tomasi corner detector (Shi and Tomasi, 1994) uses $\min(\lambda_1, \lambda_2)$ as measure of feature point. For example, Fig.7 shows a feature point detection using Harris operator for photographed image. The Harris operator detects the corner point mainly from the image as a feature point.

The position of feature point is estimate able by related position information of an artificial marker to feature point from camera image after coordinate transformation. The flight control area of RC helicopter can be expanded(see Fig.8) by using the information of natural feature points around an artificial marker. Harris operator is suitable for detecting natural points. Our system saves the areas including the natural feature points as templates when the artificial marker is detected. In the range that can take the image of the artificial marker, the system uses the position information of the artificial marker. If the system can't take the image of an artificial marker, the position of the helicopter is estimated by template matching between the area of natural feature points and the template area.

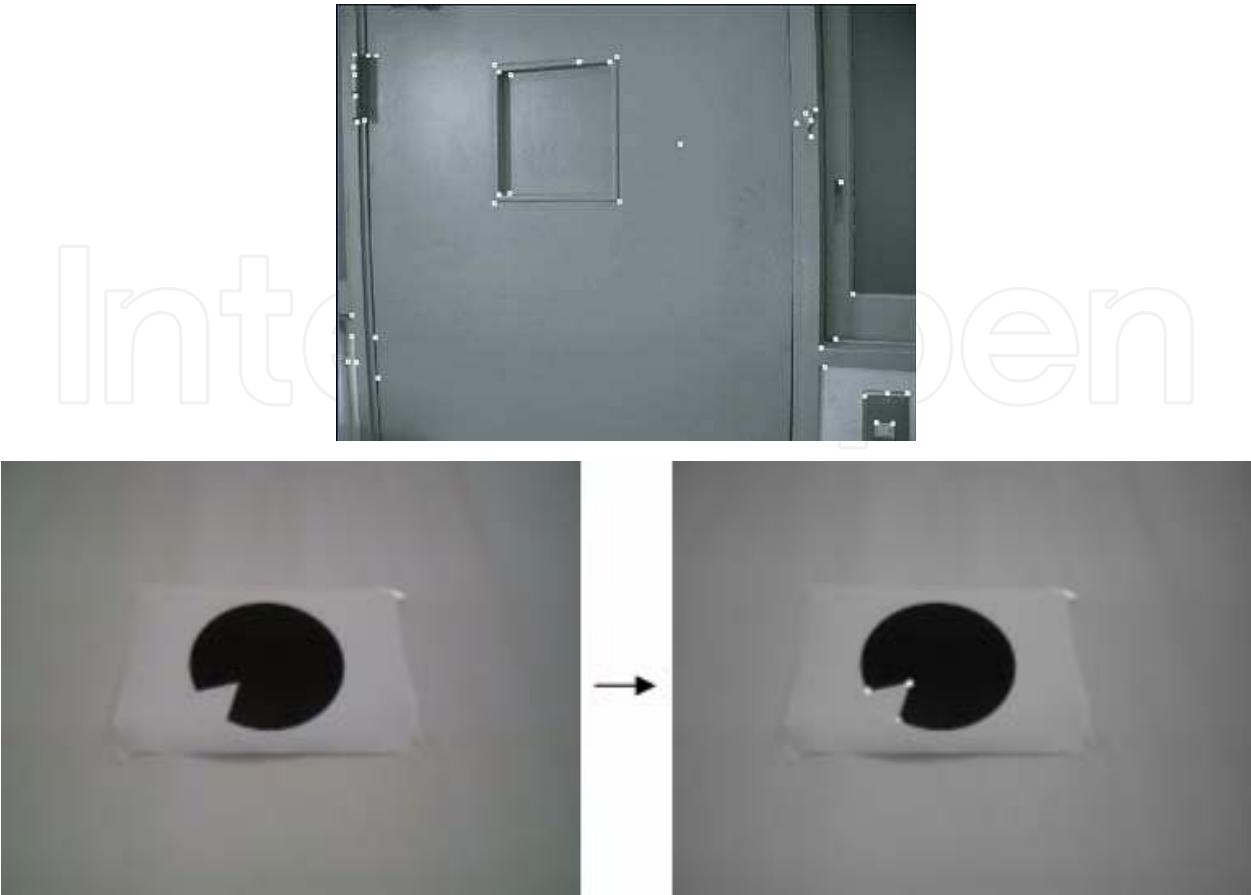


Fig. 7. Feature point extraction by a Harris operator

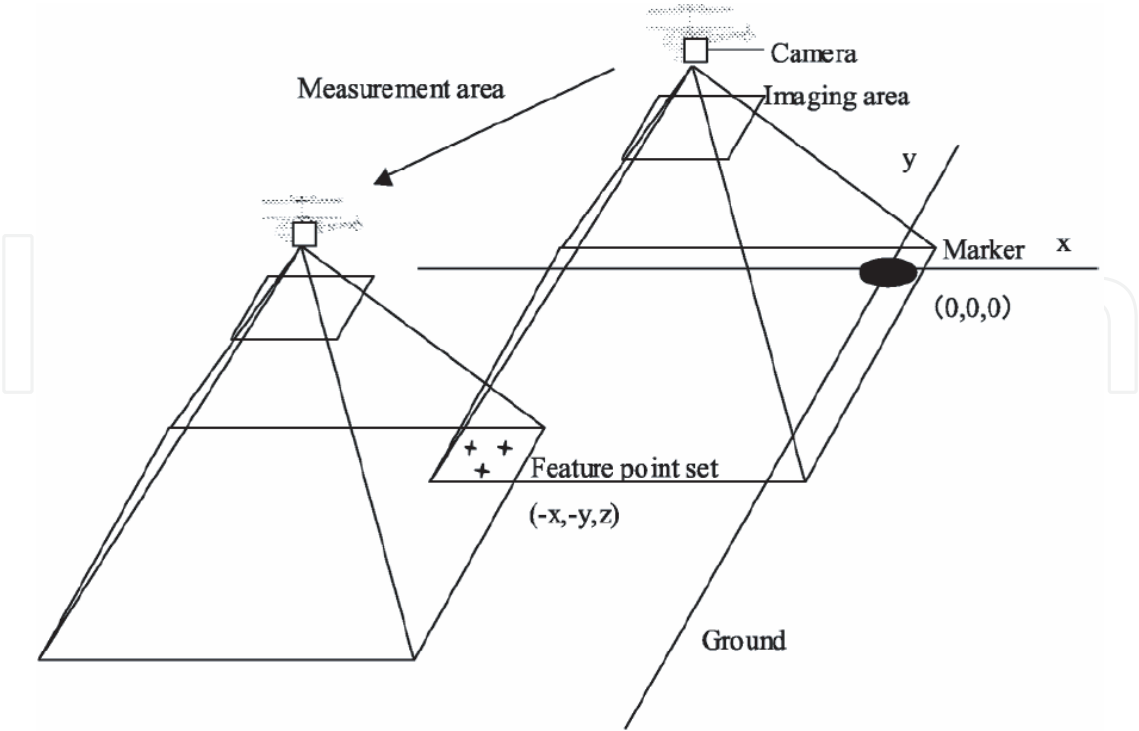


Fig. 8. The expansion of flight area

3.3 Detection of a marker

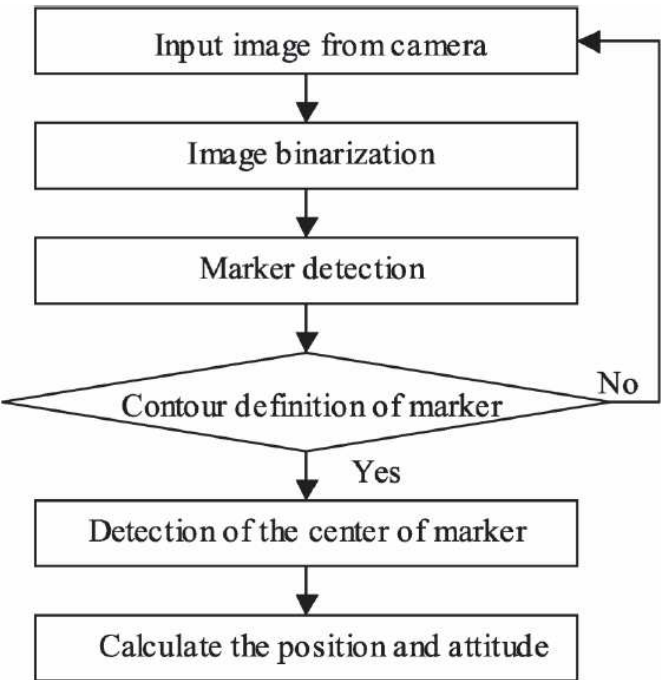


Fig. 9. The flow chart of marker detection

The image of the marker photographed with the wireless camera on micro RC helicopter is shown in Fig.4. The yaw angle can be calculated by the center of the marker and a position of a cut of triangle of the marker, and the angle of the pitch and the angle of roll can be acquired by coordinate transformation between a camera coordinate system and a world coordinate system. The flow chart about the image processing for the marker extraction and the calculation of position and posture are shown in Fig.9. First, a binarization processing is performed at the input image from the camera installed on the micro RC helicopter. Then, the marker in the image is searched, and the outline of the marker is extracted. If the outline cannot be extracted, an image is acquired from the camera again and a marker is searched again. A marker center is searched after the outline of a marker is extracted. The method of search is shown in Fig.10. The maximum values and the minimum values about the x-coordinate and y-coordinate are searched from of the extracted outline, and their middle values are given as the coordinates of the marker center. A length of major axis and a length of minor axis of the marker are calculated by the distance between the center coordinates of the marker and the pixel on the outline of the marker. The calculation method of the major axis and a minor axis is shown in Fig.11. When the center coordinate is defined as $P(x_c, y_c)$, and the coordinate of the pixel which is on the outline is defined as $I(x, y)$, the distance PI from the center to the pixel of the outline is calculated by equation (4).

$$PI = \sqrt{(x - x_c)^2 + (y - y_c)^2} \tag{4}$$

For obtaining the maximum value G_1 of PI and the minimum value G_2 of PI , all pixels on the outline are calculated. And the segment of G_1 is defined as the major axis PO , and the segment of G_2 is defined as a minor axis PQ . The position and posture of the micro RC helicopter are calculated by the method shown in Section 4.

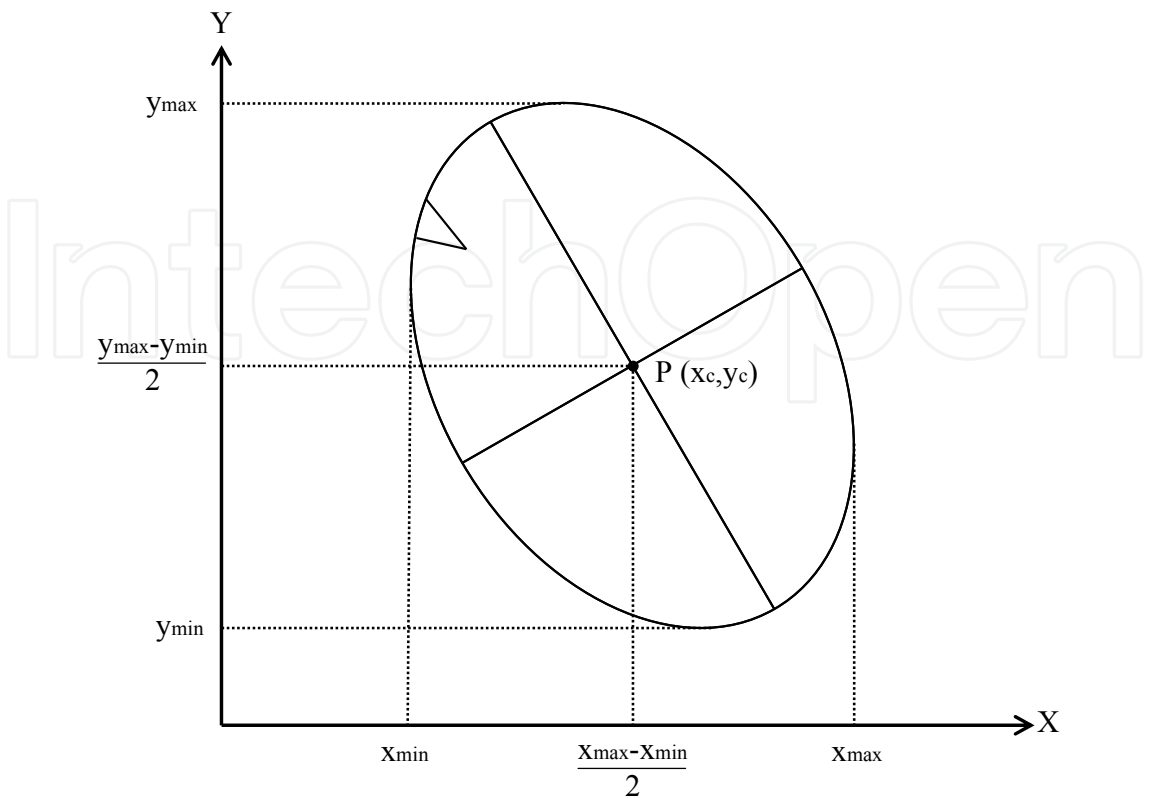


Fig. 10. The marker center

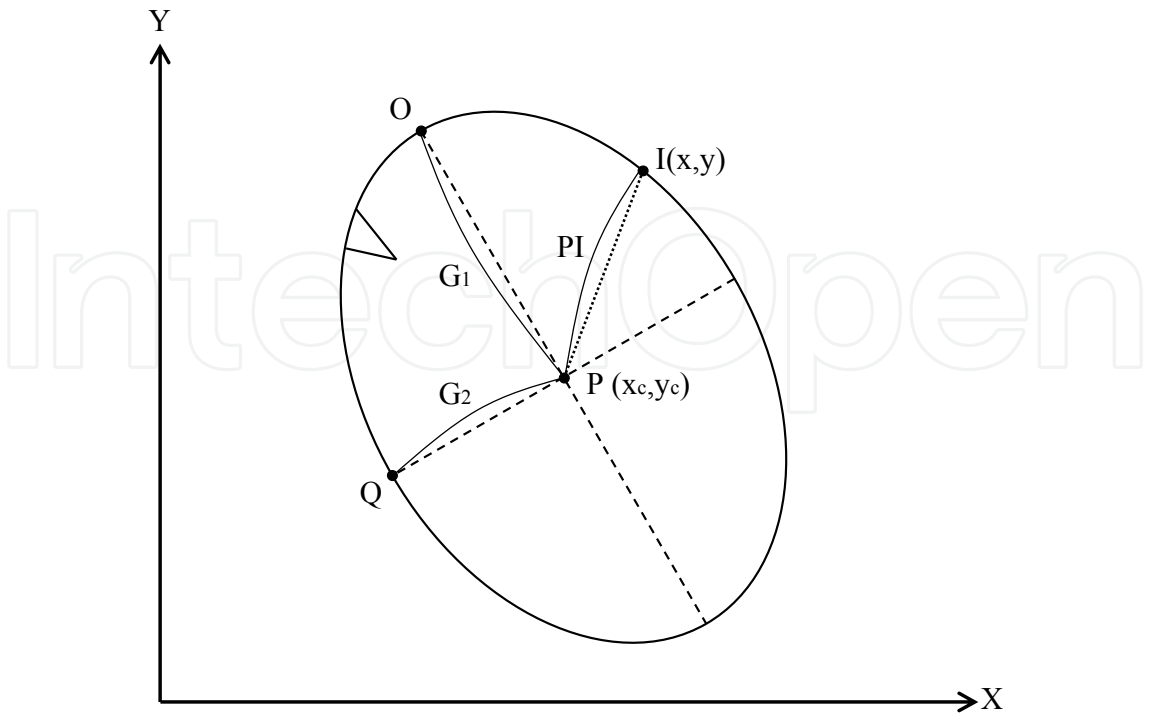


Fig. 11. The calculation method of the major axis and the minor axis of the marker

Since the vibration of the RC helicopter is quicker than the frame rate of the camera, when the camera which attached on the micro RC helicopter takes the image, the taken image has become a blurred image resulting from the interlace like Fig.6. Therefore, an exact result cannot be obtained by a usual image processing. The image processing that we devised scans with skipping the odd (or even) number lines only about y axial direction at pixel scanning. The method of scanning is shown in Fig.12. If the pixels processed are on odd lines, the even number lines are skipped only about y axial direction. About x axial direction, the system scans 1 pixel at a time like the usual pixel scanning. By this method, a stable profile tracking can be performed without being blurred by interlace.

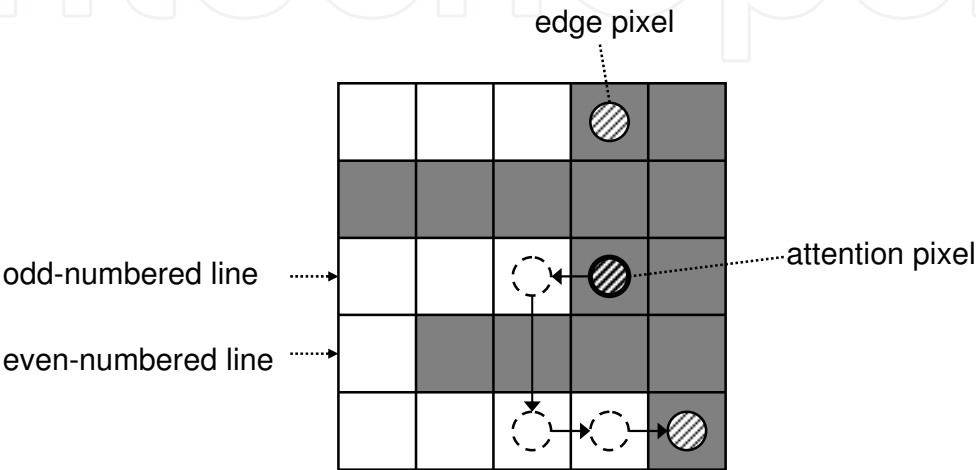


Fig. 12. The method of outline tracking

4. Calculation of position and posture

4.1 Calculation of the position coordinates of RC helicopter

In order to measure the position of the RC helicopter, it is necessary to calculate the focal distance of the wireless camera on the RC helicopter first. If the size of marker and the location of z axial direction of RC helicopter are got, the focal distance f of the wireless camera can be calculated easily. The three-dimensional coordinates of a moving RC helicopter are calculated by using the focal distance, a center of gravity and the value of radius of the marker. The image formation surface of the camera and the circular marker surface are parallel if RC helicopter is hovering above the circular marker like Fig.13.

Let's consider that a marker is in the center of the photographed image. The radius of circular marker in the camera image is defined as D_1 , and the center coordinates of the circle marker are defined as (x_{C1}, y_{C1}) . The radius of the actual marker is defined as d_1 , and the center coordinates of the actual marker in a world coordinate system are defined as (x_1, y_1, z_1) . Then, the focal distance f of a camera can be calculated from the following two equations from parallel relation.

$$z_1 : d_1 = f : D_1 \tag{5}$$

$$f = \frac{z_1 \cdot D_1}{d_1} \tag{6}$$

When the RC-helicopter is in moving, the radius of the marker in the image after moving is defined as D_2 , the center coordinates of the marker after moving are defined as (x_{C2},y_{C2}) , and the center coordinates of actual marker is defined as (x_2,y_2,z_2) . Then, the following equation is acquired.

$$z_2 : d_1 = f : D_2 \tag{7}$$

Here, since the focal distance f and the radius d_1 of actual marker are not changing, the following relation is obtained from equation (5) and equation (7).

$$D_1 : D_2 = z_2 : z_1 \tag{8}$$

z_2 can be acquired by the following equation. Moreover, x_2 and y_2 can be calculated by the following equations from parallel relation. Therefore, the coordinate of the helicopter after moving is computable by using equation (9), equation (10), and equation (11), using the focal distance of the camera.

$$z_2 = \frac{D_1 \cdot z_1}{D_2} \tag{9}$$

$$x_2 = \frac{X_2 \cdot z_2}{f} \tag{10}$$

$$y_2 = \frac{Y_2 \cdot z_2}{f} \tag{11}$$

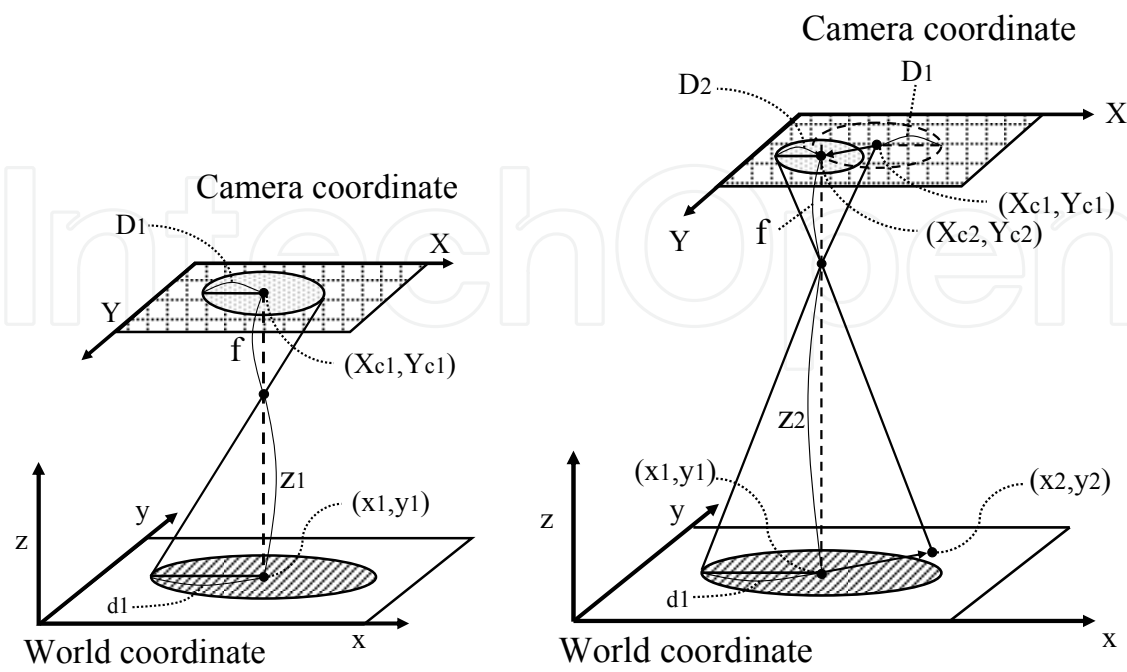


Fig. 13. The location calculation method of RC helicopter

4.2 Calculation of the attitude angle of RC helicopter

The relation between an angle of RC helicopter and an image in the camera coordinate system is shown in Fig.14. When RC helicopter is hovering above a circular marker, the circular marker image in the camera coordinate system is a right circle like an actual marker. If RC helicopter leans, the marker in a camera coordinate system becomes an ellipse. To calculate the attitude angle, first, the triangular cut part of the circular marker is extracted as a direction feature point. Then the deformation of the marker image is corrected for calculating a yaw angle using the relation between the center of the circular marker and the location of the direction feature point of the circular marker. The pitch angle and the roll angle are calculated performing coordinate transformation from the camera coordinate system to the world coordinate by using the deformation rate of the marker in the image from the wireless camera.

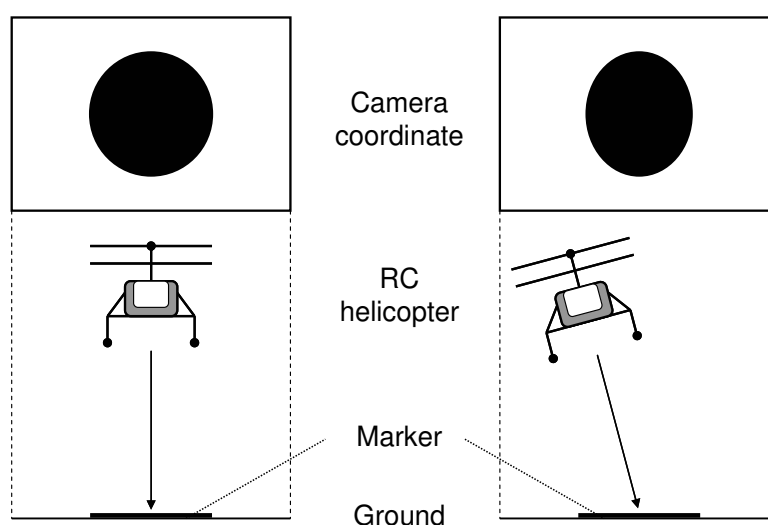


Fig. 14. Relation between attitude angle of RC helicopter and image in wireless camera.

Calculation of a yaw angle

The value of yaw angle can be calculated using the relation of positions between the center of circular marker image and the direction feature point of the circular marker image.

However, when the marker image is deforming into the ellipse, an exact value of the yaw angle cannot be got directly. The yaw angle has to be calculated after correcting the deformation of the circular marker. Since the length of the major axis of the ellipse does not change before and after the deformation of marker, the angle α between x axis and the major axis can be correctly calculated even if the shape of the marker is not corrected.

As shown in Fig.15, the center of a marker is defined as point P , the major axis of a marker is defined as PO , and the intersection point of the perpendicular and x axis which were taken down from Point O to the x axis is defined as C . The following equation is got if $\angle OPC$ is defined as α' .

$$\alpha' = \arctan\left(\frac{OC}{PC}\right) \quad (12)$$

Here, when the major axis exists in the 1st quadrant like Fig.15(a), α is equal to the value of α' , and when the major axis exists in the 2nd quadrant, α is calculated by subtracting α'

from 180 degrees like Fig.15(b). If the x -coordinate of Point O is defined as x_o , the value of α is calculated by the following equation.

$$\alpha = \begin{cases} \alpha'(x_o \geq 0) \\ 180 - \alpha'(x_o < 0) \end{cases} \tag{13}$$

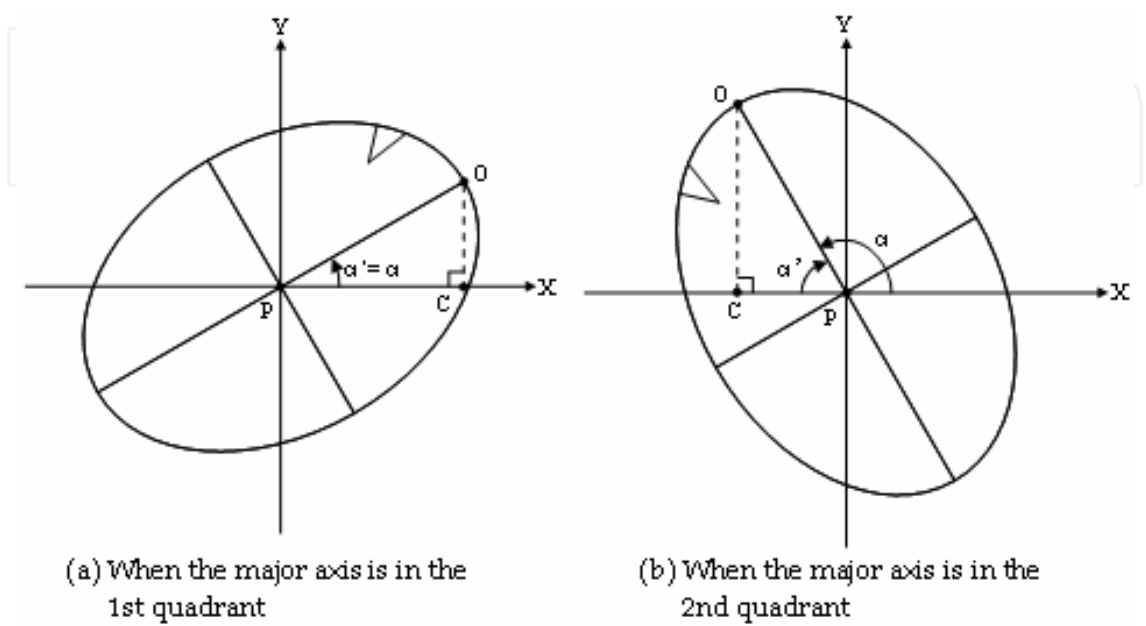


Fig. 15. An angle between the major axis and coordinate axes

Next, the angle γ between the major axis and the direction of direction feature point is calculated. When taking a photograph from slant, a circular marker transforms and becomes an ellipse-like image, so the location of the cut part has shifted compared with the original location in the circular image. The marker is corrected to a right circle from an ellipse, and the angle is calculated after acquiring the location of original direction feature point. First, the value for deforming an ellipse into a right circle on the basis of the major axis of an ellipse is calculated. The major axis of an ellipse is defined as PO like Fig.16, and a minor axis is defined as PQ . The ratio R of the major axis to a minor axis is calculated by the following equation.

$$R = \frac{PO}{PQ} = \frac{G_1}{G_2} \tag{14}$$

If this ratio multiplies along the direction of a minor axis, an ellipse can be transformed to a circle. The direction feature point of the marker in the ellipse is defined as a , and the point of intersection formed by taking down a perpendicular from Point a to the major axis PO is defined as S . If the location of the feature point on the circle is defined as A , point A is on the point of intersection between the extended line of the segment aS and a right circle. Because aS is a line segment parallel to a minor axis, the length of a line segment aS is calculated by the following equations.

$$AS = aS \times R \tag{15}$$

When the line segment between Point A and the center of the marker is defined as PA , the angle γ which the line segment PA and the major axis PO make is calculated by the following equations.

$$\gamma = \arctan \frac{AS}{PS} \quad (16)$$

Finally, a yaw angle is calculable by adding α to γ .

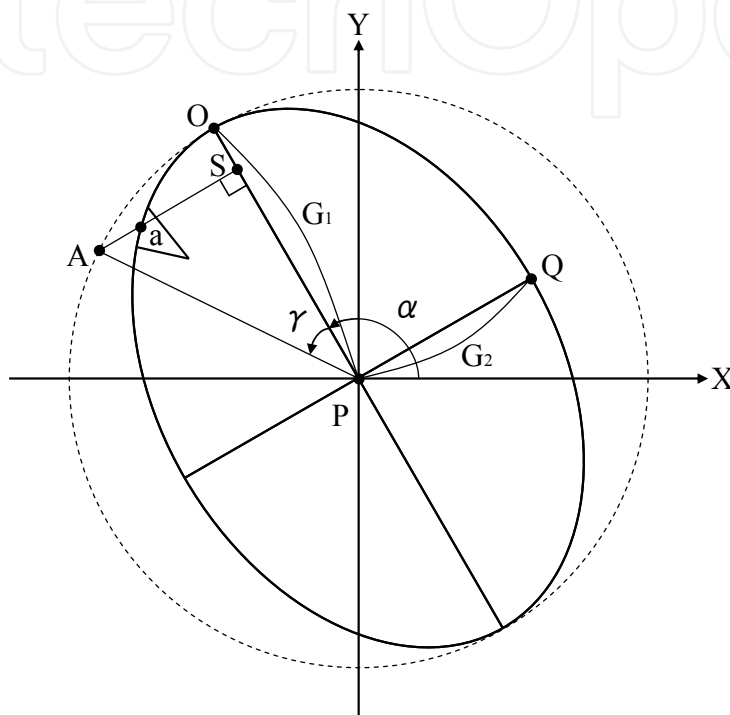


Fig. 16. An angle between the direction feature point and the major axis

Calculation of pitch angle and roll angle

By using the deformation rate of the marker in an image, a pitch angle and a roll angle can be calculated by performing coordinate transformation from a camera coordinate system to a world coordinate system. In order to get the pitch angle and rolling angle, we used a weak perspective projection for the coordinate transformation (Bao et al., 2003).

Fig.17 shows the principle of the weak perspective projection. The image of a plane figure which photographed the plane figure in a three-dimensional space by using a camera is defined as I , and the original configuration of the plane figure is defined as T . The relation between I and T is obtained using the weak perspective projection transformation by the following two steps projection.

- T' is acquired by a parallel projection of T to P paralleled to camera image surface C .
- I is acquired by a central projection of T' to C .

The attitude angle β' is acquired using relation between I and T . The angle β' shown in Fig.18 expresses the angle between original marker and the marker in the camera coordinate system. In that case, the major axis G_1 of the marker image and a minor axis G_2 of the marker image can show like Fig.19.

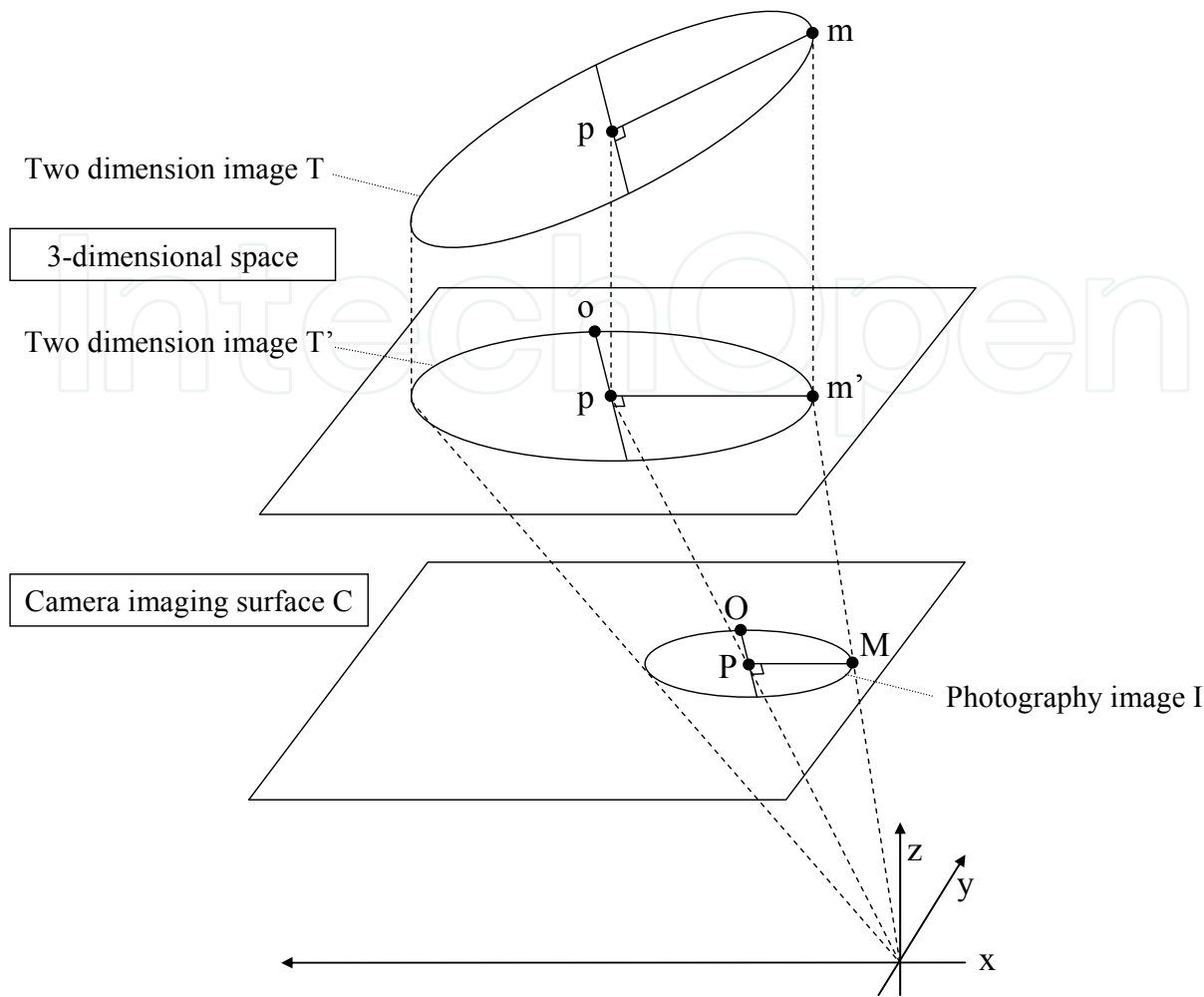


Fig. 17. The conceptual diagram of weak central projection

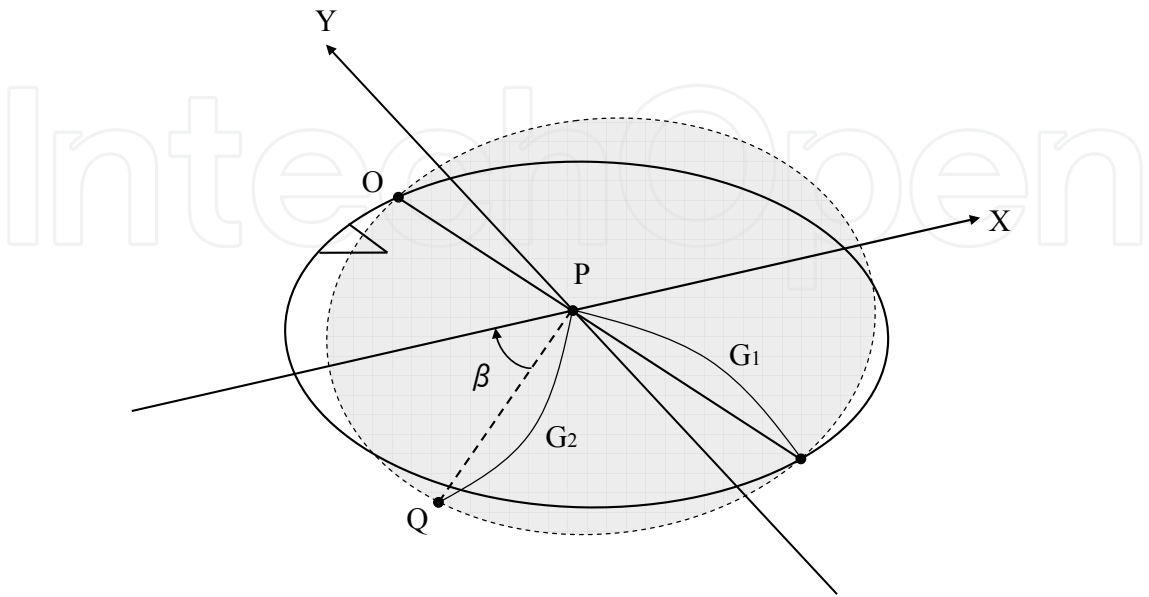


Fig. 18. The schematic diagram of the attitude angle β'

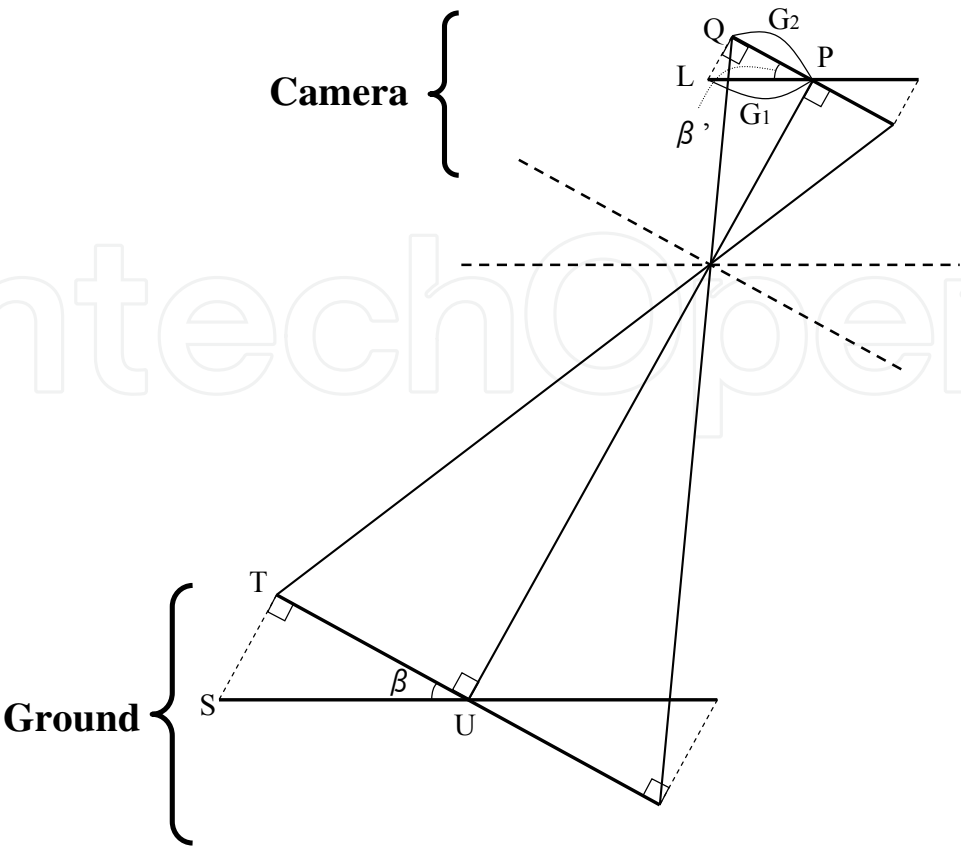


Fig. 19. Calculation of an attitude angle

Fig. 19 shows the calculation method of β' . PQ is transformed into LP if along optical axis of a camera an inverse parallel projection is performed to the minor axis PQ . Since the original configuration of a marker is a right circle, LP becomes equal to the length G_1 of the major axis in a camera coordinate system. β' is calculated by the following equation.

$$\beta' = \arcsin\left(\frac{G_2}{G_1}\right) \tag{17}$$

To get the segment TU , SU is projected orthogonally on the flat surface parallel to PQ . PQ and TU are in parallel relationship and LP and SU are also in parallel relationship. Therefore, the relation between β' and β can be shown by equation (18), and the inclination β' of the camera can be calculated by the equation (19).

$$\beta' = \beta \tag{18}$$

$$\beta = \arcsin\left(\frac{G_2}{G_1}\right) \tag{19}$$

5. Control of RC helicopter

Control of RC helicopter is performed based on the position and posture of the marker acquired by Section 4. When RC helicopter is during autonomous hovering flight, the position

data of RC helicopter are obtained by tracking the marker from definite height. The fuzzy rule of the Throttle control input signal during the autonomous flying is defined as follows.

- If $z(t)$ is PB and $\dot{z}(t)$ is PB, Then Throttle is NB
- If $z(t)$ is PB and $\dot{z}(t)$ is ZO, Then Throttle is NS
- If $z(t)$ is PB and $\dot{z}(t)$ is NB, Then Throttle is ZO
- If $z(t)$ is ZO and $\dot{z}(t)$ is PB, Then Throttle is NS
- If $z(t)$ is ZO and $\dot{z}(t)$ is ZO, Then Throttle is ZO
- If $z(t)$ is ZO and $\dot{z}(t)$ is NB, Then Throttle is PS
- If $z(t)$ is NB and $\dot{z}(t)$ is PB, Then Throttle is ZO
- If $z(t)$ is NB and $\dot{z}(t)$ is ZO, Then Throttle is PS
- If $z(t)$ is NB and $\dot{z}(t)$ is NB, Then Throttle is PB

The fuzzy rule design of Aileron, Elevator, and Rudder used the same method as Throttle. Each control input $u(t)$ is acquired from a membership function and a fuzzy rule. The adaptation value ω_i and control input $u(t)$ of a fuzzy rule are calculated from the following equations.

$$\omega_i = \prod_{k=1}^n \mu_{Aki}(x_k) \quad (20)$$

$$u(t) = \frac{\sum_{i=1}^r \omega_i c_i}{\sum_{i=1}^r \omega_i} \quad (21)$$

Here, i is the number of a fuzzy rule, n is the number of input variables, r is the quantity of a fuzzy rule, μ_{Aki} is the membership function, x_k is the adaptation variable of a membership function, and c_i is establishment of an output value (Tanaka, 1994) (Wang et al., 1997).

6. Experiments

In order to check whether parameter of a position and a posture can be calculated correctly, we compared actual measurement results with the calculation results by several experiments. The experiments were performed indoors. In the first experiment, a wireless camera shown in Fig.20 is set in a known three-dimensional position, and a marker is put on the ground like Fig.21.

The marker is photographed by this wireless camera. A personal computer calculated the position and the posture of this wireless camera and compared the calculated parameters with the actual parameters.

Table 1 shows the specification of the wireless camera and Table 2 shows the specification of the personal computer. A marker of 19cm radius is used in experiments because it is considered that the marker of this size can be got easily when this type of wireless camera which has the resolution of 640x480 pixels photographs it at a height between 1m and 2m.

Table 3 shows experimental results of z axis coordinates. Table 4 shows experimental results of moving distance. Table 5 shows experimental results of yaw angle ($\beta' + \gamma$). Table 6 shows experimental results of β' angle. According to the experimental results, although there are some errors in these computed results, these values are close to actual measurement.



Fig. 20. The wireless camera



Fig. 21. The first experiment

Maker	RF SYSTEM lab.
Part number	Micro Scope RC-12
Image sensor	270,000pixel , 1/4 inch , color CMOS
Lens	φ0.8mm Pin lens
Scan mode	Interlace
Effective distance	30m
Time of charging battery	About 45 minutes
Size	15×18×35(mm)
Weight	14.7g

Table 1. The specification of the wireless camera

Maker	Hewlett Packard
Model name	Compaq nx 9030
OS	Windows XP
CPU	Intel Pentium M 1.60GHz
Memory	768MB

Table 2. The specification of PC

Actual distance (mm)	800	1000	1200	1400
Calculated value	785	980	1225	1372

Table 3. The experimental results of z axis coordinates

Actual moving distance (mm)	50	-50	100	-100
Computed value of x axis coordinates	31	-33	78	-75
Computed value of y axis coordinates	29	-33	101	-89

Table 4. The experimental results of moving distance

Actual degree (degree)	45	135	225	315
Calculated value	64	115	254	350

Table 5. The experimental results of yaw angle (α angle + γ angle)

Actual degree (degree)	0	10	20	40
Calculated value	12	28	36	44

Table 6. The experimental results of β angle

In next experiment, we attached the wireless camera on RC helicopter, and checked if parameters of a position and a posture would be calculated during the flight. Table 7 shows the specification of RC helicopter used for the experiment. A ground image like Fig.22 is photographed with the wireless camera attached at RC helicopter during the flight. The marker is detected by the procedures of Fig.9 using image processing program. A binarization was performed to the inputted image from the wireless camera and the outline on the marker was extracted like Fig. 23. The direction feature point was detected from the image of the ground photographed by the wireless camera like Fig.24. Fig. 25 shows the measurement results on the display of a personal computer used for the calculation. The measurement values in Fig.25 were x-coordinate=319, y-coordinate=189, z-coordinate = 837, angle α =10.350105, angle γ = -2.065881, and angle β' =37.685916. Since our proposal image input method which can improve blurring was used, the position and the posture were acquirable during flight. However, since the absolute position and posture of the RC helicopter were not measureable by other instrument during the flight. We confirmed that by the visual observation the position and the posture were acquirable almost correctly.

Length	360mm(Body) , 62mm(Frame)
Width	90mm
Height	160mm
Gross load	195g
Diameter of a main rotor	350mm
Gear ratio	9.857:1
Motor	XRB Coreless Motor

Table 7. The specification of RC helicopter



Fig. 22. An image photographed by the wireless camera

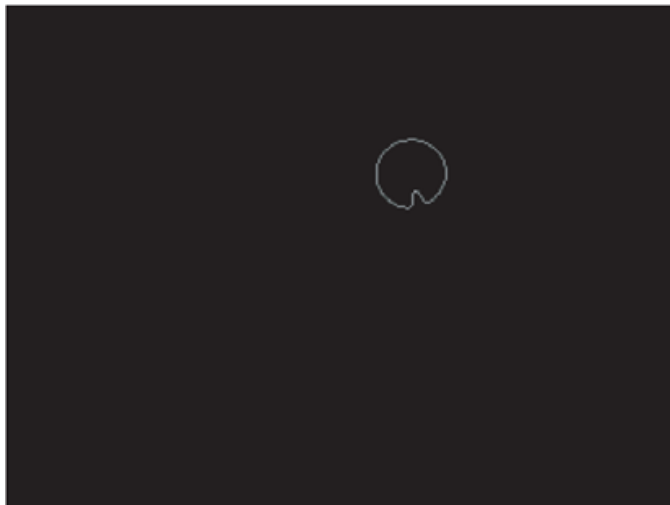


Fig. 23. The result of marker detection



Fig. 24. The result of feature point extraction

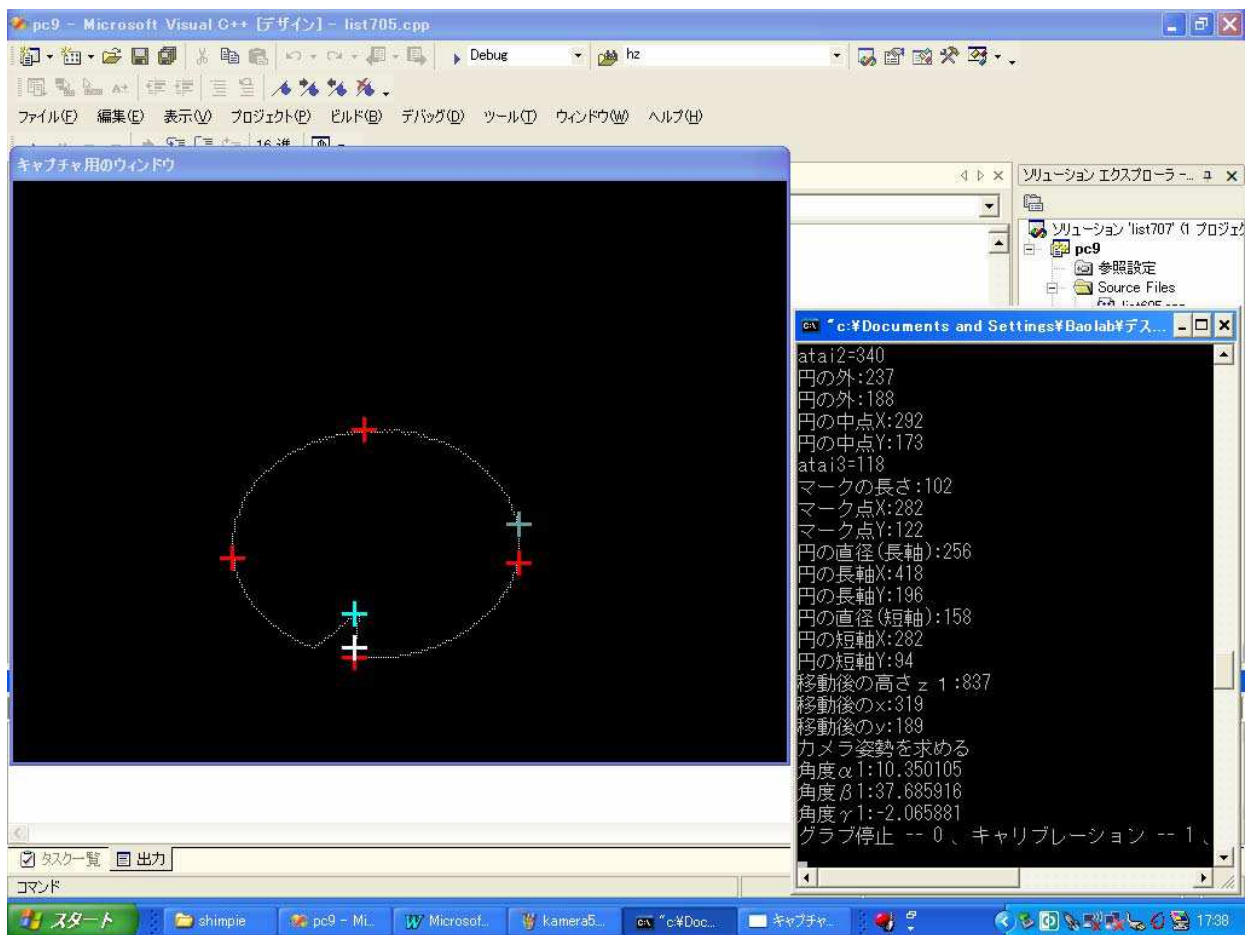


Fig. 25. The measurement results during flight

At the last, the autonomous flight control experiment of the RC helicopter was performed by detecting the marker ,calculating the position and the posture,and fuzzy control. Fig. 26 shows a series of scenes of a hovering flight of the RC helicopter. The results of image processing can be checked on the display of the personal computer. From the experimental results, the marker was detected and the direction feature point was extracted correctly during the autonomous flight. However, when the spatial relation of the marker and the RC helicopter was unsuitable, the detection of position and posture became unstable, then the autonomous flight miscarried. We will improve the performance of the autonomous flight control for RC helicopter using stabilized feature point detection and stabilized position estimation.

7. Conclusion

This Chapter described an autonomous flight control for micro RC helicopter to fly indoors. It is based on three-dimensional measuring by a micro wireless camera attached on the micro RC helicopter and a circular marker put on the ground. First, a method of measuring the self position and posture of the micro RC helicopter simply was proposed. By this method, if the wireless camera attached on the RC helicopter takes an image of the circular marker, a major axis and a minor axis of the circular marker image is acquirable. Because this circular marker has a cut part, the direction of the circular marker image can be

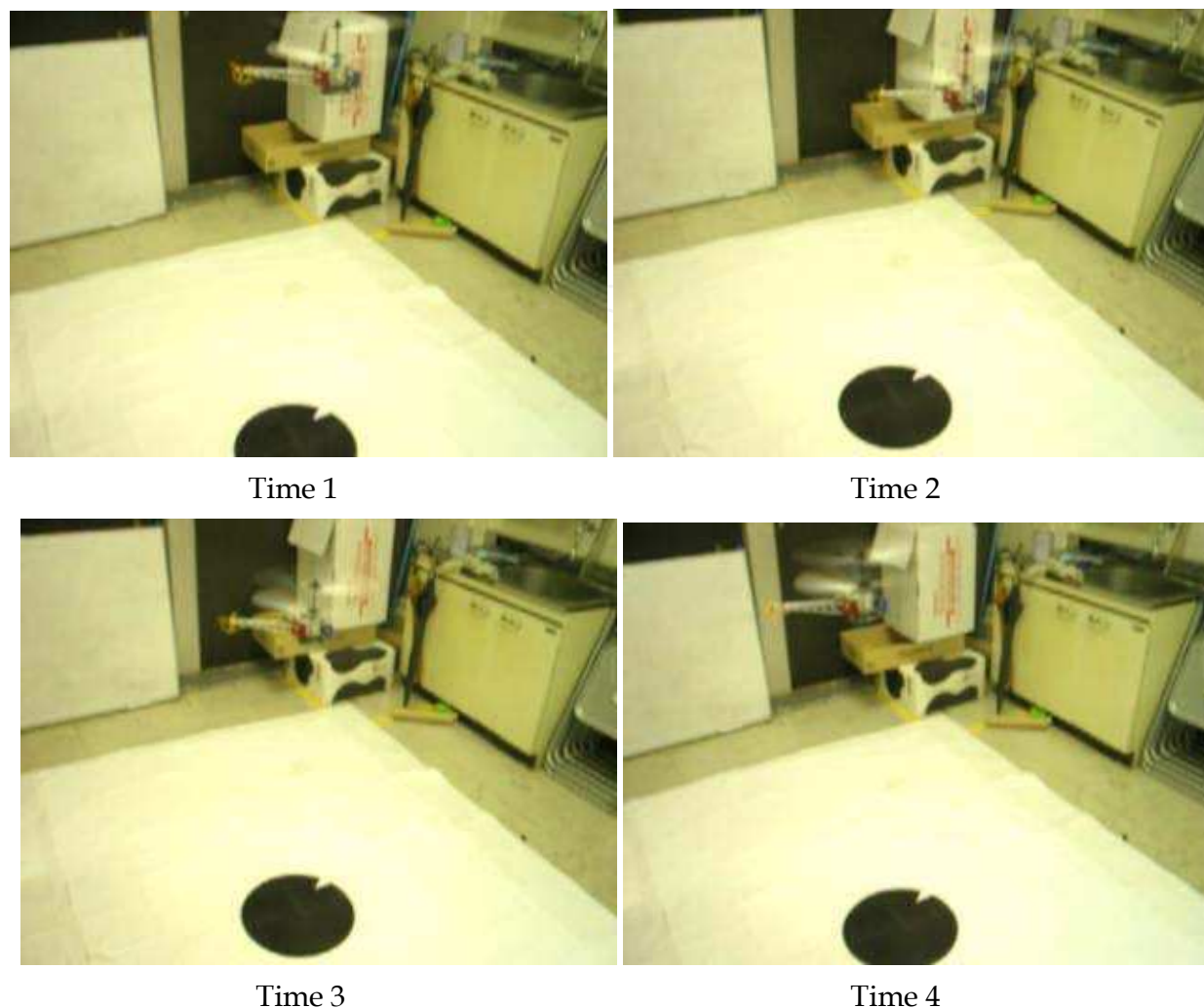


Fig. 26. The experiment of autonomous flight

acquired by extracting the cut part as a direction feature point of the circular marker. Therefore, the relation between the circular marker image and the actual circular marker can be acquired by a coordinate transform using the above data. In this way, the three-dimensional self position and posture of the micro RC helicopter can be acquired with image processing and weak perspective projection. Then, we designed a flight control system which can perform fuzzy control based on the three-dimensional position and posture of the micro RC helicopter. The micro RC helicopter is controlled by tracking the circle marker with a direction feature point during the flight.

In order to confirm the effectiveness of our proposal method, in the experiment, the position and the posture were calculated using an image photographed with a wireless camera fixed in a known three-dimensional position. By the experiment results, the calculated values near the actually measuring values were confirmed. An autonomous flight control experiment was performed to confirm that if our proposal image input method is effective when using a micro wireless camera attached on the micro RC Helicopter. By results of the autonomous flight control experiment of the RC helicopter, the marker was detected at real-time during the flight, and it was confirmed that the autonomous flight of the micro RC helicopter is possible. However, when the spatial relation of the marker and the RC helicopter was

unsuitable, the detection of position and posture became unstable and then the autonomous flight miscarried. We will improve the performance of autonomous flight control of the RC helicopter to more stable. We will improve the system so that the performance of the autonomous flight control of the RC Helicopter may become stability more.

8. Reference

- Amida, O.; Kanade, T. & Miller, J.R. (1998). Vision-Based Autonomous Helicopter Research at Carnegie Mellon Robotics Institute 1991-1997, *American Helicopter Society International Conf. Heli*, Japan.
- Harris, C. & Stephens, M. (1988). A Combined Corner and Edge Detector, *Proc. 4th Alvey Vision Conf.*, pp.147-151.
- Nakamura, S.; Kataoka, K. & Sugeno, M. (2001). A Study on Autonomous Landing of an Unmanned Helicopter Using Active Vision and GPS, *J.RSJ* Vol.18, No.2, pp.252-260.
- Neumann, U. & You, S. (1999). Natural Feature Tracking for Augmented-reality, *IEEE Transactions on Multimedia*, Vo.1, No.1, pp.53-64.
- Ohtake, H.; Iimura, K. & Tanaka, K. (2009). Fuzzy Control of Micro RC Helicopter with Coaxial Counter-rotating Blades, *journal of Japan Society for Fuzzy Theory and Intelligent Informatics*, Vol.21, No.1, pp.100-106.
- Schmid, C.; Mohr, R. & Bauckhage, C. (1998). Comparing and Evaluating Interest Points, *Proc. 6th Int. Conf. on Computer Vision*, pp.230-235.
- Shi, J. & Tomasi, C. (1994). Good Features to Track, *Proc. IEEE Conf. Comput. Vision Patt. Recogn.*, pp.593-600.
- Smith, S. M.; & Brady, J. M. (1997). SUSAN - A New Approach to Low Level Image Processing, *Int. J. Comput. Vis.*, vol.23, no.1, pp.45-78.
- Sugeno, M. et al. (1996). Intelligent Control of an Unmanned Helicopter based on Fuzzy Logic., *Proc. of American Helicopter Society 51st Annual Forum.*, Texas.
- Tanaka, K. (1994). *Advanced Fuzzy Control*, Kyoritsu Shuppan Co.,LTD, Japan.
- Wang, G.; Fujiwara, N. & Bao, Y. (1997). Automatic Guidance of Vehicle Using Fuzzy Control. (1st Report). Identification of General Fuzzy Steering Model and Automatic Guidance of Cars., *Systems, Control and Information*, Vol.10, No.9, pp.470-479.
- Bao, Y.; Takayuki, N. & Akasaka, H. (2003). Weak Perspective Projection Invariant Pattern Recognition without Gravity Center Calculation, *journal of IIEEJ*, Vol.32, No.5, pp.659--666
- Bao, Y. & Komiya, M. (2008). An improvement Moravec Operator for rotated image, *Proc. of the ADVANTY 2008 SYMPOSIUM*, pp.133-138.



Advances in Flight Control Systems

Edited by Dr. Agneta Balint

ISBN 978-953-307-218-0

Hard cover, 296 pages

Publisher InTech

Published online 11, April, 2011

Published in print edition April, 2011

Nonlinear problems in flight control have stimulated cooperation among engineers and scientists from a range of disciplines. Developments in computer technology allowed for numerical solutions of nonlinear control problems, while industrial recognition and applications of nonlinear mathematical models in solving technological problems is increasing. The aim of the book *Advances in Flight Control Systems* is to bring together reputable researchers from different countries in order to provide a comprehensive coverage of advanced and modern topics in flight control not yet reflected by other books. This product comprises 14 contributions submitted by 38 authors from 11 different countries and areas. It covers most of the current main streams of flight control researches, ranging from adaptive flight control mechanism, fault tolerant flight control, acceleration based flight control, helicopter flight control, comparison of flight control systems and fundamentals. According to these themes the contributions are grouped in six categories, corresponding to six parts of the book.

How to reference

In order to correctly reference this scholarly work, feel free to copy and paste the following:

Yue Bao, Syuhei Saito and Yutaro Koya (2011). Autonomous Flight Control for RC Helicopter Using a Wireless Camera, *Advances in Flight Control Systems*, Dr. Agneta Balint (Ed.), ISBN: 978-953-307-218-0, InTech, Available from: <http://www.intechopen.com/books/advances-in-flight-control-systems/autonomous-flight-control-for-rc-helicopter-using-a-wireless-camera>

INTECH
open science | open minds

InTech Europe

University Campus STeP Ri
Slavka Krautzeka 83/A
51000 Rijeka, Croatia
Phone: +385 (51) 770 447
Fax: +385 (51) 686 166
www.intechopen.com

InTech China

Unit 405, Office Block, Hotel Equatorial Shanghai
No.65, Yan An Road (West), Shanghai, 200040, China
中国上海市延安西路65号上海国际贵都大饭店办公楼405单元
Phone: +86-21-62489820
Fax: +86-21-62489821

© 2011 The Author(s). Licensee IntechOpen. This chapter is distributed under the terms of the [Creative Commons Attribution-NonCommercial-ShareAlike-3.0 License](https://creativecommons.org/licenses/by-nc-sa/3.0/), which permits use, distribution and reproduction for non-commercial purposes, provided the original is properly cited and derivative works building on this content are distributed under the same license.

IntechOpen

IntechOpen